

# Dynamical Arrest in Attractive Colloids: The Effect of Long-Range Repulsion

Andrew I. Campbell, Valerie J. Anderson, Jeroen S. van Duijneveldt, and Paul Bartlett  
*School of Chemistry, University of Bristol, Bristol BS8 1TS, UK.*

(Dated: September 5, 2018)

We study gelation in suspensions of model colloidal particles with short-ranged attractive and long-ranged repulsive interactions by means of three-dimensional fluorescence confocal microscopy. At low packing fractions, particles form stable equilibrium clusters. Upon increasing the packing fraction the clusters grow in size and become increasingly anisotropic until finally associating into a fully connected network at gelation. We find a surprising order in the gel structure. Analysis of spatial and orientational correlations reveals that the gel is composed of dense chains of particles constructed from face-sharing tetrahedral clusters. Our findings imply that dynamical arrest occurs via cluster growth and association.

Systems far from equilibrium often exhibit complex structures even while their equilibrium behavior may be quite mundane. A dramatic example of this phenomenon is the behavior of suspensions of attractive spherical particles which at equilibrium phase separate but which, when concentrated rapidly, form a disordered arrested solid – a ‘gel’ – able to support a weak external stress [1]. Although particle gels, formed from colloids or concentrated protein solutions, play an important role in many areas of materials science as well as biology the molecular mechanism of gelation remains far from understood [2]. Recently, in an attempt to understand the origin of the arrested states which hinder protein crystallization, attention has focused [3, 4, 5, 6, 7, 8] on gelation in systems where short-range attractions (which favor particle aggregation) are complemented by weak long-ranged repulsions (which provide a stabilizing mechanism against gelation). Experiments [3, 4, 5, 6] and simulation [7] reveal rather unexpectedly a phase of stable, freely-diffusing clusters of particles. The appearance of an equilibrium cluster fluid has lead to suggestions [7, 8] that gelation in these systems occurs via a cluster glass transition, where clusters (as opposed to particles) are trapped within repulsive cages generated by the long-range repulsion.

In this letter, we explore experimentally the effect of weak long-range repulsive forces on dynamical arrest in a model system of uniform colloids with short-range attractions. We use three-dimensional fluorescence confocal microscopy to follow the process of gelation directly with single particle resolution. In sharp contrast with the structure of all gel networks studied to date, we find that the connected solid network exhibits a high degree of orientational ordering. Our findings suggest that kinetic arrest occurs via a one-dimensional cluster growth and percolation mechanism and not a cluster glass transition as has been proposed previously [7, 8].

Our particles are poly(methyl methacrylate) [PMMA] spheres stabilized against aggregation by a thin ( $\sim 10$ nm) covalently-bound layer of poly(12-hydroxystearic acid). The spheres have a mean radius of  $a = 777$  nm, a polydispersity of 3% about the mean, a mass density of

$\rho_c = 1.176$  g cm $^{-3}$  and are labelled with the fluorescent dye DiIC $_{18}$  [9]. The spheres are dispersed in a mixture of cycloheptyl bromide (CHB) and *cis*-decalin, which nearly matches both the mass density and the index of refraction of the colloid. In this mixture the PMMA spheres have a small but reproducible positive charge. Phase sensitive electrophoretic light scattering measurements reveal a net charge  $Q$  of  $+140e$  on each particle, equivalent to a surface charge density  $\sim 10^{-6}$  that of typical aqueous colloids.

The potential between spheres,  $U(r)$ , is the sum of long-ranged screened coulombic repulsions  $U_{LR}(r)$  and a short-ranged attractive potential,  $U_{SR}(r)$ . The electrostatic repulsion has the familiar Yukawa form,  $U_{LR}(r) = (A/r) \exp[2\kappa a(1-r)]$ . Here the Debye length  $\kappa^{-1}$  reflects the effective range of the coulombic repulsions screened by the ions in solution,  $r$  is the pair distance between particles scaled by the diameter  $2a$  and  $A$  is the contact value of the potential.  $\kappa^{-1}$  is considerably extended by comparison to aqueous systems as a result of the low solubility of ions. We estimate the ionic strength as around  $5 \times 10^{-9}$  mol dm $^{-3}$ , corresponding to a Debye screening length  $\kappa^{-1} = 1 \pm 0.2\mu\text{m}$  [10]. The potential at contact,  $A$ , was estimated from electrophoretic measurements as  $+30k_B T$ . To induce particle aggregation we generate a short-range attraction between particles by adding poly(styrene), a non-adsorbing polymer. We use a polymer with a mean molecular weight of  $10^7$  Daltons and a mean radius of gyration  $r_g \approx 92$  nm. The attractive interactions induced occur at pair separations less than  $\xi = r_g/a$  or approximately 13% of the colloid diameter. Their strength is controlled by the polymer concentration and is equal to  $U_{SR}/k_B T \approx -14\phi_p$  at contact, assuming the polymer behaves ideally; here  $\phi_p$  is the fraction of the *free* volume of solution occupied by polymer coils. Again, we emphasize the markedly different range of the attractive and repulsive potentials; the attractions act on a length scale  $\xi a$  while the repulsions extend over a scale  $\kappa a \gg \xi a$ .

To study the three-dimensional structure of particle gels we use fluorescence confocal microscopy. The suspension was contained in a cylindrical reservoir 10 mm in

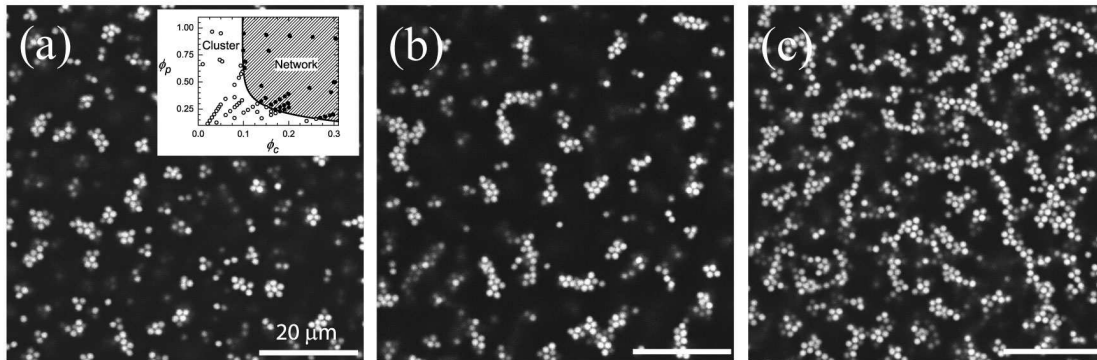


FIG. 1: Confocal microscope images of colloid-polymer mixtures at different volume fractions. From left to right:  $\phi_c = 0.080$ ,  $0.094$ , and  $0.156$ . The attractive interactions are the same in all samples,  $U_{SR} = -9k_B T$  ( $\phi_p = 0.69$ ). Images (a) and (b) contain clusters while (c) shows a network phase. The bars are  $20 \mu\text{m}$  long. Inset: Phases observed as a function of the volume fractions of colloid ( $\phi_c$ ) and polymer ( $\phi_p$ ).

diameter and  $650 \mu\text{m}$  deep created by sealing the edges of a  $170 \mu\text{m}$  coverslip to a microscope slide. Fluorescence was excited by a He-Ne laser ( $543 \text{ nm}$ ) and imaged through a  $50 \mu\text{m}$  pinhole. The digital image was optimized using the Nyquist criterion to select pixel size and frame spacing from the instrumental resolution. The microscope's  $63\times$  oil immersion objective provided a field of view of  $73 \times 73 \mu\text{m}^2$  with a magnification of  $71 \text{ nm/pixel}$ . Typically,  $345$  vertically spaced images were collected at a separation of  $0.16 \mu\text{m}$ . Three-dimensional particle coordinates were extracted with an accuracy of about  $50 \text{ nm}$  using algorithms similar to those described in [11].

Confocal microscopy images of colloid-polymer mixtures at fixed attraction  $U_{SR} = -9 k_B T$  and three different particle concentrations are shown in Fig. 1. At the lowest volume fraction (Fig. 1a) the sample contains a fluid of small, approximately spherical clusters. We confirmed that the clusters were stable by repeatedly imaging the sample for over a week, observing no significant growth in the size of clusters. With increasing  $\phi_c$  the clusters grow in extent, becoming less spherical and more chain-like; the micrographs (Fig. 1b) collected 4 hours after loading clearly show short strands of densely packed chains of particles with a relatively uniform thickness ( $\sim 2a$ ). The orientation and center of mass of each strand fluctuates and the sample is ergodic. Finally, at high densities ( $\phi_c > 0.1$ ) the clusters form a connected solid network, which Fig. 1c reveals occurs with no change in local structure; the gel consists of linked densely-packed chains of particles, reminiscent of percolation. Although the long-range structure of the network is highly disordered, there is a surprising degree of uniformity at short scales. The chains which form the network are clearly of nearly equal thickness. Repeated scanning reveals that while individual chains display local fluctuations all long-range motion is suppressed and the sample is nonergodic. Using confocal visualization we followed the transition between the ergodic cluster fluid and nonergodic network

as both the colloid density  $\phi_c$  and the short-range attractions  $U_{SR}$  were varied. A well-defined boundary between the two phases is clearly evident (inset, Fig. 1) which we identify as the gelation transition.

The spatial correlations evident in the gel are intriguing. The order is in sharp contrast to all previous reports of colloidal gels where the structure has been characterized locally either as a scale-invariant fractal cluster (e.g. [5]) or, less commonly, as an amorphous packing of hard spheres [12]. The confocal images confirm that the local order is not a consequence of gelation. The same local structure is clearly present in both the fully ergodic cluster fluid (near the gelation boundary) as well as the non-ergodic gel. Indeed the main change at gelation is the degree to which chains are interconnected rather than any change in their internal structure. Thus we hypothesize that a weak long-range repulsion coupled with a short-ranged attraction favors the formation of dense strands of particles, the length of which grow with increasing  $\phi_c$  until, at the gelation transition, the strands become completely interconnected and a gel forms. To test this hypothesis we determine the three-dimensional coordinates of our samples. We focus on the gels formed with attractive interactions fixed at  $U_{SR} = -13 k_B T$ , referring to future publications for a more extensive analysis.

We first provide numerical evidence of correlations that are independent of density and characteristic of the chains that form the network. We start by analyzing the translational order present. From the particle coordinates we compute the pair correlation function  $g(r)$  and hence the local density profile  $\phi(r) = \frac{24\phi_c}{r^3} \int_0^r s^2 g(s) ds$ , which is the average volume fraction within a sphere of radius  $r$  centered on each particle. Fig. 2(a) shows  $\phi(r)$  evaluated for different gel densities. The local volume fraction decays rapidly towards  $\phi_c$  on distances of  $3-4$  particle diameters, indicating that translational order is short-ranged at all volume fractions. The situation is very different at shorter scales ( $r \approx 2a$ ) where transla-

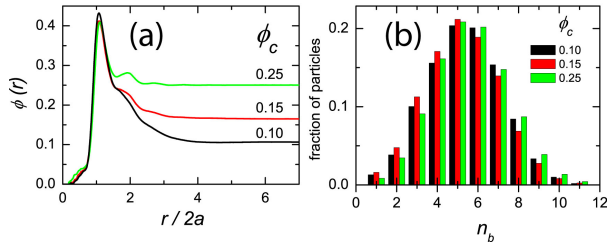


FIG. 2: Correlations in colloidal gels as a function of  $\phi_c$  (a) The local volume fraction  $\phi(r)$  and (b) the proportion of particles bonded to  $n_b$  neighboring particles. Note that the peak in  $\phi(r)$  at  $r = 2a$  is independent of volume fraction and the distribution of particles bonds does not change with  $\phi_c$ .

tional order is enhanced; on these scales Fig. 2(a) indicates that the local environment is dense and essentially independent of  $\phi_c$ ; the ‘cage’ around each particle has a volume fraction  $\sim 0.5$  (from the peak of  $\phi(r)$ ) and a size  $\approx 2a$ . To probe further the local organization we examine the orientational order. We define particles which are ‘bonded’ to each other by their separation  $r$ . If  $r \leq r_0$ , where  $r_0$  is identified with the position of the first minimum in  $g(r)$ , then the particles are considered neighbors. This definition ensures that all particles in the first coordination shell are counted as near neighbors. Fig. 2(b) shows the distribution in the number of bonds per particle as the gel density is varied. The bond distribution is essentially independent of  $\phi_c$ , confirming the picture of the gel as a network of invariant chains. The mean number of bonds per particle is  $n_b = 5.6 \pm 0.4$ , midway between the values of 2–3 expected for a fractal structure and the 12 bonds found in dense liquids and glasses. More dramatic evidence for the three-dimensional order within the gel is shown in Fig. 3, which shows a two-dimensional projection of particle centers and bonds identified within a small slab of gel. The image reveals that the gel consists of relatively uniform chains constructed from dense clusters of particles.

To check for local tetrahedral coordination we calculate the rotational invariants  $q_l(i)$ ,  $\hat{w}_l(i)$  (for  $l = 4$  and  $6$ ), which are quantitative measures of the local bond topology around particle  $i$ . We define the bond-order parameters following [13]. Structural and thermal fluctuations result in a distribution of  $q_4$ ,  $q_6$ ,  $\hat{w}_4$  and  $\hat{w}_6$ . The resulting bond-order distributions provide a sensitive measure of the symmetry of the local environment [13]. The  $\hat{w}_6$ -distribution, in particular, facilitates the detection of structures with tetrahedral symmetry since a large negative value signals a high degree of tetrahedral order. A tetrahedral cluster has  $\hat{w}_6 = -0.106$  while an icosahedron, an ordered arrangement of twenty tetrahedra, maximizes  $|\hat{w}_6|$  at  $\hat{w}_6 = -0.170$  [14]. By contrast, the cubic symmetries found in *fcc*, *hcp* and *bcc* crystals lead to near zero values of  $\hat{w}_6 = -0.013$ ,  $-0.012$ , and  $0.013$  respectively.

Figure 4 shows the bond-order histograms measured

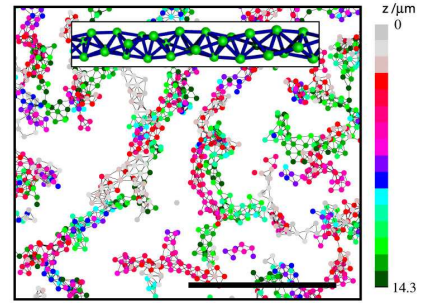


FIG. 3: A two-dimensional projection of the particle centers within a slab of gel ( $14.3 \mu\text{m}$  deep) at  $\phi_c = 0.1$ . Particles are colored as a function of their depth within the sample and drawn 40% of their actual size for clarity. The bar is  $20 \mu\text{m}$  long. Inset: A spiral chain formed from tetrahedra of particles sharing faces.

for the gel at  $\phi_c = 0.10$  (the distributions obtained at other densities were similar but are not shown). The pronounced maximum in the  $\hat{w}_6$ -distribution at  $\hat{w}_6 \sim -0.13$  is particularly striking and demonstrates a high degree of orientational order. The peak is at too low a value however to be accounted for by tetrahedral units alone and the small number of bonds per particle is incompatible with an icosahedral symmetry. Although neither structure is consistent with the data, the position of the  $\hat{w}_6$  maximum, intermediate between the values expected for tetrahedral and icosahedral clusters, suggests that the gel probably contains *ordered* clusters of tetrahedra.

Polytetrahedral order has been invoked to understand the structure of quasicrystals, atomic liquids and glasses [15, 16, 17] however the concept has not been applied to gels, as far as we know. A viable structure must account for the chains evident in the confocal images together with the strong propensity for six-fold coordination found experimentally. These constraints eliminate many possibilities. So for example, while linear chains of edge- or corner-sharing tetrahedra are common motifs in structural chemistry the number of bonds per particle varies along the chain and averages out at less than 6. More dense tetrahedral chains can be built by sharing *faces* of neighboring tetrahedral units. There is a single dimer of two face-sharing tetrahedra with the symmetry of a trigonal bipyramid, one trimer (a bicapped tetrahedron), two distinct tetramers and five pentamers. The number of such arrangements grows rapidly as more tetrahedral units are added so that an infinite sequence of face-sharing tetrahedra may exist in any one of an infinite number of possible configurations, each with a different chain contour. Each configuration however has an identical shell of six nearest neighbors since the neighbors of each particle belong to a trimer of adjacent tetrahedra, which may be realized in only one way. Here we focus on the most striking configuration, the graceful Bernal [15] (or Boerdijk-Coxeter [18, 19]) spiral, reproduced in Fig. 3. We have calculated the distributions of bond-

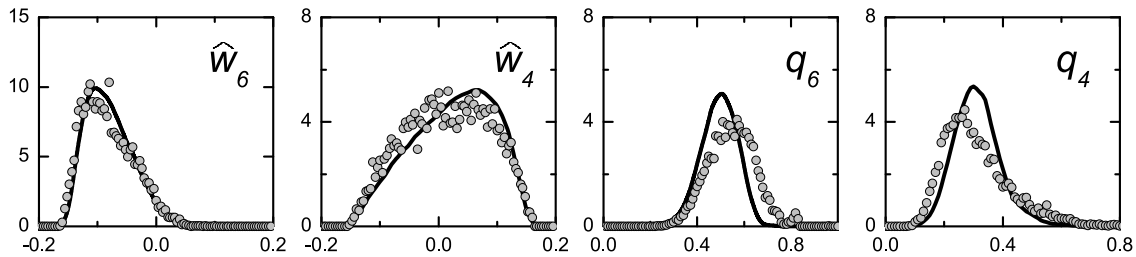


FIG. 4: Orientational order in a colloidal gel with  $\phi_c = 0.10$  and  $U_{SR} = -13k_B T$ . Measured  $\hat{w}_6$ ,  $\hat{w}_4$ ,  $q_6$  and  $q_4$  bond-order parameter distributions (points) together with values calculated from a model of face-sharing tetrahedra (black curves).

order parameters from computer-generated coordinates for a spiral strand consisting of 1000 tetrahedra. Thermal and structural fluctuations were simulated by adding random deviations, chosen from a Gaussian distribution of width  $\Delta a$ , to the ideal coordinates. Fig. 4 depicts the bond-order distributions calculated for the Bernal spiral with  $\Delta = 0.21$  where it is clear the measured  $\hat{w}_6$ - and  $\hat{w}_4$ -histograms are reproduced rather well by this model, strongly supporting our picture of the gel as a network constructed from chains of face-sharing tetrahedra. The measured  $q_6$ - and  $q_4$ -distributions are less well reproduced but this is probably linked to the fact that our model only has six-fold coordinated species while the measurements contain particles with both more and fewer than 6 nearest neighbors.

In summary, we have shown that the mechanism of dynamical arrest is profoundly altered by the presence of long-range repulsive interactions. Three-dimensional confocal microscopy reveals the formation of stable chain-like clusters, constructed from face-sharing tetrahedral units, which associate into a fully connected network at gelation. The possibility that a delicate balance of attraction and long-range repulsion may stabilize equilibrium clusters has been discussed in recent theoretical work [20, 21]. However it is not clear if the formation of tetrahedra reflects the presence of charge or is simply a consequence of a centro-symmetric attractive potential. An explanation for the unexpected structures seen in our experiments remains an open challenge to theorists. Finally it is tempting to draw analogies between the one-dimensional growth seen here and the tendency to chain formation observed in several protein solutions [22, 23]. These similarities suggest that weakly-charged colloidal systems could offer valuable new insights into the microscopic mechanism of protein nucleation and gelation.

We thank Macolm Faers, Adele Donovan and Laura Starrs for extensive discussions and help during the experiments. This work was supported by EPSRC, Bayer Cropsciences and MCRTN-CT-2003-504712.

- 
- [1] K. A. Dawson, *Curr. Opin. Colloid Interf. Sci.* **7**, 218 (2002).
  - [2] See, e.g. *Non-Equilibrium Behavior of Colloidal Dispersions, Edinburgh, UK, 2002*, [Faraday Discuss. **123** (2003)].
  - [3] A. Stradner, H. Sedgwick, F. Cardinaux, W. C. K. Poon, S. Egelhaaf, and P. Schurtenberger, *Nature* **432**, 492 (2004).
  - [4] H. Sedgwick, S. Egelhaaf, and W. C. K. Poon, *J. Phys. Condens. Matter* **16**, S4913 (2004).
  - [5] A. D. Dinsmore and D. A. Weitz, *J. Phys. Condens. Matter* **14**, 7581 (2002).
  - [6] P. N. Segre, V. Prasad, A. B. Schofield, and D. A. Weitz, *Phys. Rev. Lett.* **86**, 6042 (2001).
  - [7] F. Sciortino, S. Mossa, E. Zaccarelli, and P. Tartaglia, *Phys. Rev. Lett.* **93**, 055701 (2004).
  - [8] K. Kroy, M. E. Cates, and W. C. K. Poon, *Phys. Rev. Lett.* **92**, 148302 (2003).
  - [9] A. I. Campbell and P. Bartlett, *J. Colloid Interface Sci.* **256**, 325 (2002).
  - [10] The ionic strength was determined from the measured sample conductivity ( $170 \text{ pS cm}^{-1}$ ) assuming ion diffusivities of 6 and  $2 \times 10^{-10} \text{ m}^2 \text{ s}^{-1}$ , typical of  $\text{Br}^-$  and alkyl cation diffusion. The Debye length was calculated at  $\phi_c = 0.1$ , allowing for the screening from the solvent ions and the  $Q$  counter-ions associated with each particle.
  - [11] J. C. Crocker and D. G. Grier, *J. Colloid Interface Sci.* **179**, 298 (1996).
  - [12] P. Varadan and M. J. Solomon, *Langmuir* **19**, 509 (2003).
  - [13] P. R. ten Wolde, M. J. Ruiz-Montero, and D. Frenkel, *J. Chem. Phys.* **104**, 9932 (1996).
  - [14] P. J. Steinhardt, D. R. Nelson, and M. Ronchetti, *Phys. Rev. B* **28**, 784 (1983).
  - [15] J. D. Bernal, *Proc. Royal Soc. (London) A* **280**, 299 (1964).
  - [16] D. R. Nelson, *Solid State Phys.* **42**, 1 (1989).
  - [17] J. P. K. Doye and D. J. Wales, *Phys. Rev. Lett.* **86**, 5719 (2001).
  - [18] A. H. Boerdijk, *Philips Res. Bull.* **7**, 303 (1952).
  - [19] H. S. M. Coxeter, *Can. Math. Bull.* **28**, 385 (1985).
  - [20] S. Mossa, F. Sciortino, P. Tartaglia, and E. Zaccarelli, *Langmuir* **20**, 10756 (2004).
  - [21] J. Groenewold and W. K. Kegel, *J. Phys. Chem. B* **105**, 11702 (2001).
  - [22] M. Weijers, R. W. Visscher, and T. Nicolai, *Macromol.* **35**, 4753 (2002).
  - [23] C. Le Bon, T. Nicolai, and D. Durand, *Int. J. Food Sci.*

and Technology **34**, 451 (1999).